



Managed aquifer recharge and exploitation impacts on dynamics of groundwater level 1 2 and quality in northern China karst area: Quantitative research by multi-methods 3 4 Han Cao<sup>1,2</sup>, Jinlong Qian<sup>1,2</sup>, Huanliang Chen<sup>3,4</sup>, Chunwei Liu<sup>3,4</sup>, Minghui Lyu<sup>3,4</sup>, Shuai Gao<sup>3,4</sup>, Weihong Dong<sup>1,2,\*</sup>, Caiping Hu<sup>3,4,\*</sup> 5 6 7 <sup>1</sup> Key Laboratory of Groundwater Resources and Environments, Ministry of Education, Jilin University, 8 Changchun, People's Republic of China <sup>2</sup> Institute of Water Resources and Environment, Jilin University, Changchun, People's Republic of 10 China 11 <sup>3</sup> 801 Institute of Hydrogeology and Engineering Geology, Shandong Provincial Bureau of Geology & 12 Mineral Resources, Jinan, China 13 <sup>4</sup> Shandong Engineering Research Center for Environmental Protection and Remediation on 14 Groundwater, Jinan, China 15 16 Corresponding Author: dongweihong@jlu.edu.cn, caipinghu126@126.com 17 **Abstract** 18 19 Managed aquifer recharge (MAR) is an effective way to counter groundwater level decline and 20 spring depletion caused by excessive groundwater exploitation in karst areas. However, the unique 21 characteristics of karst groundwater systems make the groundwater quantity and quality more susceptible 22 to human activities, posing challenges for MAR research. This research employed multi-methods 23 including numerical simulations, isotope analysis, infiltration tests, flow monitoring and tracer tests to 24 quantitatively analyze the impacts of MAR and groundwater exploitation on the dynamics of https://doi.org/10.5194/egusphere-2025-281 Preprint. Discussion started: 10 February 2025 © Author(s) 2025. CC BY 4.0 License.





25 groundwater level and quality in a typical northern China karst area, the Baotu Spring area in Jinan 26 City. First, the percentage of surface water recharge in karst groundwater was calculated using isotope 27 data with the improved two-end-member mixing model. Next, the quantitative relationship between 28 volume of released water and actual recharge was established with data from infiltration tests and flow 29 monitoring. Then, the actual groundwater flow velocity and effective porosity of the karst aquifers were 30 calculated with former tracer test isochrone maps. Finally, the impacts of MAR and groundwater 31 exploitation on dynamics of groundwater level and quality were quantitatively analyzed with a 32 groundwater flow-solute transport model for the area. The results indicate that the MAR and groundwater 33 exploitation in the Baotu Spring area have significantly impacted karst groundwater levels and quality. 34 These complementary methods enhance the accuracy of decisions in MAR and groundwater exploitation. 35 Keywords: Managed aquifer recharge (MAR); Karst groundwater; Quantitative analysis; Multi-methods. 36 1. Introduction 37 Managed aquifer recharge (MAR) (Sherif et al., 2023), refers to the intentional recharge of aquifers 38 to address the ecological and environmental geological issues caused by excessive groundwater 39 exploitation (Aeschbach-Hertig & Gleeson, 2012; Foley et al., 2011). It has been demonstrated that 40 appropriate recharge can effectively elevate groundwater levels and improve groundwater quality to 41 some extent (Ajjur & Baalousha, 2021; Alam et al., 2021; Standen et al., 2020). 42 Karst groundwater is a crucial component of water resources (Hartmann et al., 2014; Medici et al., 43 2021). The research of MAR in karst areas has become a prominent focus in recent years (J. Li et al., 44 2023; Zhang & Wang, 2021). However, the unique characteristics of karst groundwater systems make 45 the groundwater quantity and quality more susceptible to human activities (Allocca et al., 2014; Lorenzi 46 et al., 2024), posing challenges for MAR research. Due to the highly heterogeneous nature of karst

https://doi.org/10.5194/egusphere-2025-281 Preprint. Discussion started: 10 February 2025 © Author(s) 2025. CC BY 4.0 License.





47 development, the actual effectiveness of MAR varies significantly across different locations (Daher et 48 al., 2011). The impact of recharge on the karst groundwater level and quality at different locations and 49 using various water sources shows significant variation. Additionally, the fast karst groundwater flow 50 (Bakalowicz, 2005) leads to extensive catchment areas for karst groundwater exploitation wells, and 51 over-exploitation would create large-scale groundwater level drawdown cones, causing secondary 52 geological hazards (Jiang et al., 2019). Moreover, if poor-quality source water were used for MAR, 53 pollutants would quickly spread downstream (H. Cao et al., 2023), severely threatening the quality of 54 karst groundwater (Xanke et al., 2017). Therefore, quantitatively assessing the effects of MAR and 55 groundwater exploitation on the quantity and quality of karst groundwater will facilitate stable, efficient, 56 and safe aquifer recharge and groundwater exploitation. 57 There are some relatively mature research methods regarding the effects of MAR and groundwater 58 exploitation on groundwater level and quality (Ringleb et al., 2016). However, most of these methods 59 are either qualitative or semi-quantitative. Hydrogeochemical and isotope methods are commonly used 60 in MAR studies (Akurugu et al., 2022; M. Li et al., 2023). By monitoring the changes in groundwater 61 quality before and after the recharge, the impact of MAR on groundwater quality can be qualitatively 62 analyzed. A primary issue with hydrogeochemical analysis is that its conclusions may be ambiguous, as 63 potential unknown sources of groundwater contamination could interfere with the results. In addition, 64 isotopes in groundwater are often used to identify recharge sources. By combining multiple 65 hydrochemical and isotopic indicators (Guo et al., 2019), the proportion of various recharge sources 66 contributing to groundwater can be estimated (Deng et al., 2022). However, in many cases, due to the 67 inability to accurately determine the isotopic values for each recharge source, this method can only 68 provide a rough estimate. Furthermore, due to the typical lack of long-term monitoring data on





69 groundwater isotopes, this approach is unsuitable for studying the dynamics in the effects of MAR on 70 groundwater. 71 Numerical simulation is a powerful tool for quantitative research of MAR (Ghasemizadeh et al., 72 2012; Medici et al., 2021; Ostad-Ali-Askari & Shayannejad, 2021). The Equivalent Porous Medium 73 (EPM) model, represented by MODFLOW, is suitable for simulating laminar groundwater flow that 74 adheres to Darcy's law (Jourde & Wang, 2023; Ringleb et al., 2016). In karst regions with low 75 development, such as the karst areas in northern China, groundwater flow is predominantly laminar, 76 largely complying with Darcy's law (Chuanlei Li et al., 2022). Therefore, the EPM model without 77 inserting karst-conduits embedded is well-suited for application in these regions (Kang et al., 2011; J. Li 78 et al., 2023; Luo et al., 2020; Scanlon et al., 2003). 79 When conducting MAR studies using numerical simulation methods, accurately determining the 80 actual groundwater recharge volume is a crucial condition for ensuring the accuracy of the simulation 81 results. In the studies of MAR primarily driven by riverbed infiltration, methods such as riverbed 82 infiltration tests and river flow monitoring can be employed. By applying the principles of groundwater 83 dynamics and water balance, the actual surface water recharge to groundwater can be quantitatively 84 calculated. 85 Furthermore, it has been indicated that when using the EPM model for simulating solute transport 86 in karst groundwater, properly estimating the effective porosity of karst aquifers is critically important 87 (Kidmose et al., 2023; Ren et al., 2018). Overestimating the effective porosity often results in a severe 88 underestimation of the actual groundwater velocity, leading to significant errors in karst groundwater 89 pollution control measures (Medici & West, 2021; Medici et al., 2019). Therefore, to ensure the effective 90 application of the EPM model in groundwater solute transport simulating, it is advisable to consider





92 calculated from tracer tests (Worthington et al., 2019; Zhu et al., 2020). 93 In MAR studies conducted in actual regions, the results of various methods mentioned above can 94 be cross-validated to reduce the uncertainty caused by data scarcity or insufficient investigation, thereby 95 improving the accuracy of quantitative research related to MAR. 96 The Baotu Spring area in Jinan City is a typical representative of the karst areas in northern China 97 (Liang et al., 2018), with karst groundwater serving as one of the crucial water supply sources. In the 98 past decades, the increasing demand for water resources in Jinan has led to excessive groundwater 99 exploitation, causing a decline in groundwater levels and the drying up of springs (Gao et al., 2023; 100 Changsuo Li et al., 2022). In order to balance the needs of water supply and spring protection, Jinan City 101 has implemented the project of MAR using the diverted water from the Yellow River (Kang et al., 2011) 102 and the Yangtze River from the South-to-North Water Transfer Project (Liu et al., 2020) in recent years. 103 Studies have shown that there is a close hydraulic connection between surface water and karst 104 groundwater in certain reaches of the Yufu River and Xingji River, making them ideal sites for 105 implementing the MAR project (J. Li et al., 2023). However, when the flow of Yufu River is excessively 106 high, a portion of the flow downstream and cannot recharge the karst groundwater. Moreover, the 107 concentration of some hydrochemical components in the diverted water may be higher than those of the 108 local karst groundwater (X. Cao et al., 2023; J. Li et al., 2023; Zheng et al., 2020), and thus long-term 109 use of lower-quality water for recharge may lead to continuous deterioration of karst groundwater quality 110 (J. Li et al., 2023; Zhang & Wang, 2021). 111 Therefore, to ensure the stability of the karst groundwater level and the long-term safety of water 112 quality, and to guarantee the sustainable exploitation of groundwater resources, the purpose of this

estimating the effective porosity of the karst aquifer medium using the actual groundwater flow velocity

https://doi.org/10.5194/egusphere-2025-281 Preprint. Discussion started: 10 February 2025 © Author(s) 2025. CC BY 4.0 License.





research is to quantitatively analyze the impacts of MAR and groundwater exploitation on the dynamics of karst groundwater level and quality in the Baotu Spring area of Jinan City by multi-methods. The method employed in this study primarily focuses on the numerical simulation of coupled groundwater flow and solute transport. Complementary techniques such as isotope analysis, infiltration tests, flow monitoring, and tracer tests are also utilized to enhance the accuracy of the numerical simulations.

### 2. Material and methods

#### 2.1. Study area

The study area of this paper is the Baotu Spring area, located in Jinan City, Shandong Province, China, covering about 1,654 km² (Niu et al., 2021; Sun et al., 2013) (Fig.1). The terrain of Baotu Spring area is higher in the south and lower in the north, with rolling steep mountains and deep canyons in the south, low mountains and hills in the middle, and Piedmont inclined plains and alluvial plains in the north. The Baotu Spring area is located in the mid-latitude inland area with a warm temperate continental climate. The average annual precipitation from 1951 to 2023 is 690.4 mm, mostly falling between June and September (accounting for 77% of the total), and southern mountainous areas receive more precipitation than northern plains.

130

132

133

134

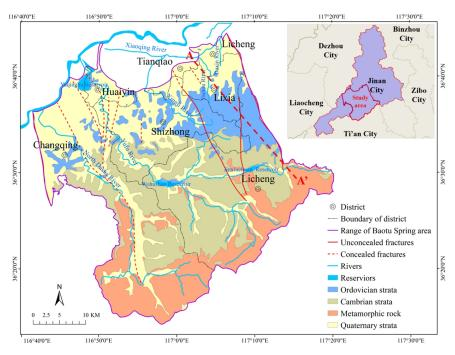
135

136

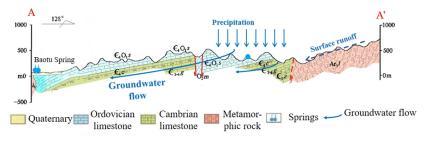
137







129 (a) Geological map



131 (b) Hydrogeological profile

Fig.1 Geological map and hydrogeological profile of Baotu Spring area

The main rivers in this region are the Yellow River, Yufu River, and Beisha River (Fig.1). The Yellow River forms the study area's northwestern boundary and is mainly used for agricultural irrigation and groundwater recharge. The Yufu River is a seasonal tributary of the Yellow River, and the reaches between Zhaiertou and Cuima Villages has excellent permeability, making it an ideal river for MAR (Guo et al., 2019; J. Li et al., 2023) (Fig.2). Additionally, the Xingji River in the northeast, though small,

139

140

141

142

143

144

145

146

147

148

149

150

151

152

153

154

155

156

157

158

159





also has a permeable riverbed making it suitable for MAR (Fig.2).

The stratigraphic units exposed in the study area from south to north, listed from oldest to youngest, are as follows: Archaean Taishan Group metamorphic rocks, Cambrian limestone, Ordovician limestone, and Quaternary loose sediments (Fig.1). The exploitable karst groundwater is stored in the Zhangxia Formation of the middle Cambrian, the Chaomidian Formation of the upper Cambrian, and the Majiagou Formation of the Ordovician. In the northern mountainous and hilly areas, karst groundwater is recharged by precipitation and surface water, flowing northward along strata dips (Zhu et al., 2020). In the northern piedmont alluvial plain, the karst aquifer is buried under Quaternary sediments. Large gabbro intrusions from the late Mesozoic block the northward flow, causing the water to rise along fractures and form springs (Niu et al., 2021; Wang et al., 2022), with Baotu Spring being the most popular of them (Guo et al., 2019). In addition, only few of the groundwater exploiting wells in the study area are still under exploitation, which could be categorized into three groups (western suburbs wells, western Jinan wells and eastern suburbs wells) based on the locations. Most of the MAR in the study area is conducted along certain river reaches of the Yufu River and Xingji River, while a small portion of the MAR is carried out through specific wells in the urban area (which are no longer used for exploitation and are now solely dedicated to MAR) (Wang et al., 2017). The locations of all these exploiting wells, MAR wells, and MAR river reaches are marked in Fig.2. 2.2. Groundwater sampling and analysis In the study area, surface water is the primary source of MAR. In order to understand the current water quality status of karst groundwater and surface water in the study area, identifying the

hydrochemical components in surface water that may influence groundwater quality, estimate the





percentage contribution of surface water and precipitation recharge to karst groundwater, and to provide a basis for the groundwater flow and solute transport model setup, sampling and analysis of groundwater and surface water in the study area were conducted in June 2022. The analyzed indicators included total dissolved solids (TDS), sulphate concentration, nitrate concentration, chloride concentration,  $\delta^2$ H‰, and  $\delta^{18}$ O‰. The locations of the sampling points are shown in Fig.2.

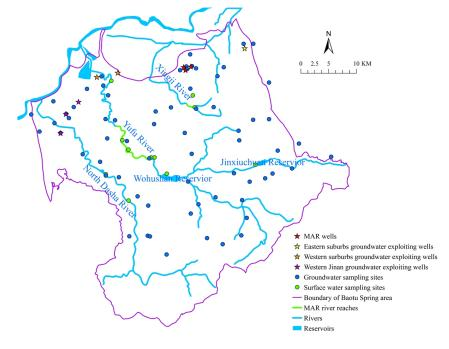


Fig.2 Locations of wells and sampling sites

After the analysis of groundwater and surface water samples, the origin and recharge sources of karst groundwater were determined by utilizing the  $\delta^2 H\%$  and  $\delta^{18}O\%$  scatter plot of groundwater and surface water. The analysis of  $^2H$  and  $^{18}O$  requires referencing the Global Meteoric Water Line (GMWL) and the Local Meteoric Water Line (LMWL). The GMWL is given as (Craig, 1961):

$$\delta^2 H = 8\delta^{18} O + 10$$
 (1)

Using the China Meteoric Water Line (CWML) as the LWML for the study area, which is:





$$\delta^2 H = 7.7 \delta^{18} O + 7 \tag{2}$$

Then, to quantitatively analyze the impact of MAR from surface water on karst groundwater,  $\delta^2 H\%$  and  $\delta^{18}O\%$  values were used to determine the proportion of groundwater recharge from surface water. Groundwater in the study area has two main recharge sources: surface water and precipitation (Liu et al., 2021). An improved two-end-member mixing model was employed to calculate the mixing ratios of surface water and precipitation in groundwater samples. Assuming  $\delta^2 H\%$  and  $\delta^{18}O\%$  values for surface water are  $x_s$  and  $y_s$ , for precipitation are  $x_p$  and  $y_p$ , and for groundwater are  $x_g$  and  $y_g$ , the mixing ratios from surface water ( $\eta_s$ ) and precipitation ( $\eta_p$ ) were calculated. The traditional two-end-member mixing

$$\begin{cases}
\eta_s = \frac{x_g - x_p}{x_s - x_p} \\
\eta_p = \frac{x_s - x_g}{x_s - x_p}
\end{cases}$$
(3)

model uses either  $\delta^2 H\%$  or  $\delta^{18} O\%$  data to calculate these ratios with the formula:

183 Or:

181

185

186

187

188

190

191

192

193

$$\begin{cases}
\eta_s = \frac{y_g - y_p}{y_s - y_g} \\
\eta_p = \frac{y_s - y_g}{y_s - y_n}
\end{cases} \tag{4}$$

For some samples, the mixing ratios calculated using formula (3) or (4) differ significantly. This paper proposes a method that calculates the mixing ratio by projecting groundwater sample points onto the precipitation-surface water mixing line in a  $\delta^2 H\% - \delta^{18} O\%$  diagram. The derived formula for calculating the mixing ratio is as follows:

189 
$$\begin{cases} \eta_{s} = \frac{(x_{g} - x_{p})(x_{s} - x_{p}) + (y_{g} - y_{p})(y_{s} - y_{p})}{(x_{s} - x_{p})^{2} + (y_{s} - y_{p})^{2}} \\ \eta_{p} = \frac{(x_{s} - x_{g})(x_{s} - x_{p}) + (y_{s} - y_{g})(y_{s} - y_{p})}{(x_{s} - x_{p})^{2} + (y_{s} - y_{p})^{2}} \end{cases}$$
(5)

In this research, the minimum  $\delta^2H\%$  and  $\delta^{18}O\%$  values of karst groundwater samples are considered as the values of precipitation recharge end-members, which are -64.56 and -9.30, respectively. The average  $\delta^2H\%$  and  $\delta^{18}O\%$  values of surface water samples are considered as the values of surface water recharge end-members, which are -50.53 and -6.815, respectively. Using formula (5), the mixing ratio

https://doi.org/10.5194/egusphere-2025-281 Preprint. Discussion started: 10 February 2025 © Author(s) 2025. CC BY 4.0 License.





for all karst groundwater samples could be calculated.

#### 2.3. Infiltration test and flow monitoring of rivers

To investigate the infiltration capacity of an MAR river reach, we selected five equidistant sites along the MAR reach of Yufu River and measured the permeability coefficient of the riverbed based on in-situ double-ring infiltration test (Li et al., 2019) (Fig.3). Then, the infiltration coefficient of the Yufu River MAR reach was calculated using the double-ring infiltration test results. The theoretical maximum recharge capacity was then determined based on the river's area.

Additionally, the flow monitoring data from multiple reaches of the Yufu River and Xingji River from 2014 to 2016 were collected (Fig.3). According to the principle of water balance, the difference in flow between the cross-sections of the MAR river reach is considered as the actual infiltration recharge volume. For Yufu River, the water is released in Section #1, and the actual infiltration recharge volume equals the difference between the flow rate at Section #1 and Section #5. For Xingji River, the water is released in Section #6, and the actual infiltration recharge volume equals the difference between the flow rate at Section #1 and Section #5. For Xingji River, the water is released in Section #6, and the actual infiltration recharge volume equals the difference between the flow rate at Section #6 and Section #7. Then, based on the statistical data of the released water volume, the

quantitative relationship between the released water volume and the actual recharge volume is analyzed.





#5
#4

#5
#6

Infiltration test sites
Flow monitoring sections
Boundary of district
Range of Baotu Spring area
MAR river reaches
Rivers
Reservoirs

Fig.3 Infiltration test sites and flow monitoring sections

## 2.4. Estimation of effective porosity from tracer tests

Effective porosity is a crucial parameter for simulating groundwater solute transport. The actual groundwater velocity determined by tracer tests can be used to calculate the effective porosity of karst fractured aquifers (Zuber & Motyka, 1994), using the following formula:

$$n_f = \frac{\kappa_{\rm I}}{v_{\rm t}} \tag{6}$$

This formula is derived based on Darcy's law. In the equation, "K" represents the hydraulic conductivity (m/d), "F" is the hydraulic gradient, and " $v_t$ " is the actual groundwater velocity. There are two large-scale tracer tests which have been conducted at Cuima village in year 1989 and in Xingji River in year 2016 (Zhu et al., 2020). To determine the parameters required in the groundwater solute transport model, the actual groundwater flow velocity and the effective porosity of the karst aquifer were calculated based on the data from the two tracer tests (Fig.4).

First, three groundwater flow lines were extracted from the groundwater flow field, and several calculation points for groundwater flow velocity and effective porosity were selected at equal intervals.





Flow lines #1 and #2 represent the diffusion direction of the tracers from Cuima Village, while flow line #3 represents the diffusion direction of the tracers from Xingji River. Using the isochrone map of tracer peak concentration diffusion, the actual groundwater flow velocity was calculated based on the horizontal distance between adjacent isochrones at each calculation point. The hydraulic gradient at the calculation points on flow lines #1 and #2 was calculated using 1989 groundwater level monitoring data, and the hydraulic gradient on flow line #3 was calculated using 2016 data. The permeability coefficient (*K*) for each calculation point was determined using the groundwater flow model established in this research. Finally, the effective porosity at each calculation point was calculated using formula (6).

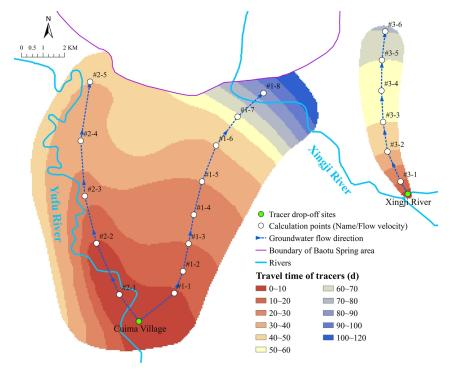


Fig.4 Tracer tests conducted in Cuima Village and Xingji River

# 2.5. Groundwater flow-solute transport simulation

Numerical simulation is used to predict groundwater level and quality in this research. As mentioned in the introduction, the EMP model without inserting karst-conduits embedded is capable for





237 groundwater flow simulation in karst regions with low development like the northern China karst areas. 238 Therefore, the GMS software was used to establish a karst groundwater flow and solute transport model 239 for the Baotu Spring area. The MODFLOW 2005 and MT3DMS packages were employed to solve the 240 groundwater flow and solute transport equations using the finite difference method. 241 The numerical model encompasses the Baotu Spring area, simplifying the stratigraphy into four 242 units: Quaternary pore phreatic aquifer, intrusive rock aquitard, Ordovician-Cambrian karst aquifer, and 243 the aquitard below the Mantou Formation (Fig. 5(a)). The Ordovician-Cambrian karst aquifer is the main 244 aquifer and the target aquifer for MAR and groundwater exploitation. The boundaries of the Ordovician-245 Cambrian karst aquifer are set as Fig.5(b). Additionally, the boundaries of other strata are all impervious. 246 The model's source and sink terms include precipitation recharge, MAR from rivers and wells, 247 groundwater exploitation, spring discharge, agricultural irrigation exploitation, and agricultural irrigation 248 re-infiltration. Precipitation recharge is calculated based on precipitation quantity, infiltration recharge 249 coefficient, and recharge zone area. The infiltration recharge coefficient considers surface lithology, 250 urbanization, and agricultural development. The MAR from rivers mainly occur through the Yufu and 251 Xingji Rivers, and the actual recharge volume is discussed in Section 3.2. The locations of MAR wells, 252 groundwater exploiting wells and MAR river reaches are displayed in Fig.5(b). 253 The hydraulic conductivity K consists of horizontal hydraulic conductivity  $K_x$  and vertical hydraulic 254 conductivity  $K_y$ . The zoning and values of  $K_x$  are mainly based on the hydrogeological tests, and then 255 identified and verified using groundwater level monitoring well data.  $K_v$  is uniformly set to 0.1 times  $K_x$ . 256 The remaining hydrogeological parameters (specific yield, storage coefficient, and dispersity) are taken 257 as empirical values. The determination of effective porosity has been discussed in Section 2.4. The 258 simulation period spans from January 1, 2020, to December 31, 2022, with each stress period lasting one

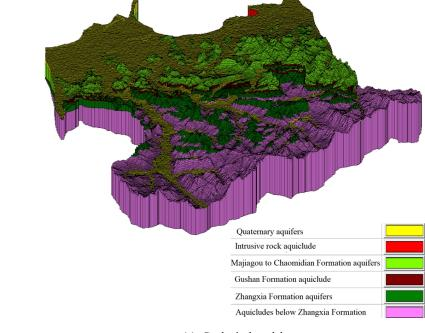




month.

Next, the impact of MAR and groundwater exploitation on the dynamics of karst groundwater levels was quantitatively analyzed using a groundwater flow model, with Baotu Spring's water level serving as a representative indicator. The considered MAR are from Yufu River, Xingji River, and MAR wells. For the simulation period of 2020-2022, the net variations of Baotu Spring water level caused by MAR and groundwater exploitation were calculated.

Finally, to quantitatively compare the effects of various MAR and groundwater exploitation on the dynamics of Baotu Spring water level, the water level net variation after 1, 2, and 3 years of continuous recharge and exploitation at a constant flow rate was calculated and compared.



(a) Geological model





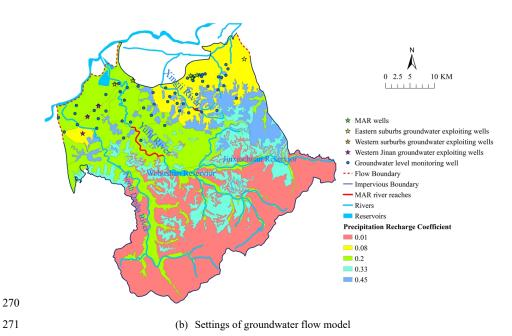


Fig.5 Geological model and groundwater flow model

For the solute transport simulation, sulphate is selected as the representative solute because its concentration in the surface water used for MAR is higher than that in the groundwater, while the concentrations of other solute components are either similar to or lower than those in the groundwater. The simulation is based on the groundwater flow model from 2020 to 2022, with all recharge/discharge values averaged over this period to mitigate seasonal flow variations. The initial sulphate concentration in karst groundwater is uniformly set at 50 mg/L, reflecting the average concentration in high-quality water from the wells in western suburbs. The model then simulates the dynamics of sulphate concentration in karst groundwater after 2, 6, and 18 months of continuous recharge with sulphate concentrations of 150 mg/L, 250 mg/L, and 350 mg/L in the MAR water.

### 3. Results and discussion

### 3.1. Mixing percentages of groundwater recharge sources

A scatter plot of the  $\delta^2H\%$  and  $\delta^{18}O\%$  of groundwater and surface water is generated in Fig.6. It





shows that karst groundwater samples are distributed near the LWML, indicating that the karst groundwater in the study area originates from precipitation (Liu et al., 2021). The isotopic enrichment of <sup>2</sup>H and <sup>18</sup>O in surface water samples is significantly higher than that in karst groundwater samples, exhibiting a typical evaporation effect. Additionally, the karst groundwater samples gradually deviate from the LMWL with the enrichment of <sup>2</sup>H and <sup>18</sup>O, indicating the mixing of precipitation and surface water. This suggests that the karst groundwater is significantly recharged by surface water.

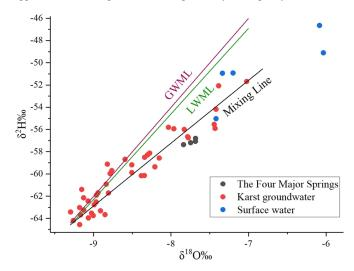


Fig.6 Scatter plot of  $\delta^2H\%$  and  $\delta^{18}O\%$  in water samples

The mixing percentage of surface water recharge in groundwater is exhibited in Fig.7. According to the result, the closer the distance to the MAR reaches of Yufu River and Xingji River, the higher the mixing percentage of surface water recharge in the groundwater. In the southern metamorphic rock and Cambrian Zhangxia Formation limestone outcrop areas, as well as the northwestern Yellow River alluvial plain, the mixing percentage of surface water recharge is generally less than 20%. In contrast, in the middle and lower reaches of the Yufu River and North Dasha River basins, as well as the Xingji River basin, the mixing percentage of surface water recharge is relatively high. The highest mixing percentage is near the MAR reaches of the Yufu River and Xingji River. For example, in the villages





along the MAR reach of the Yufu River, the mixing percentage of surface water recharge in wells ZhaiET, Cui1, and J97 exceeds 80%, while in wells A2-30 and Ji1 near the Xingji River MAR reach, and the Springs downstream, it exceeds 50%. These results highlight that the MAR from the Yufu River and Xingji River is a significant component of karst groundwater resources, emphasizing the importance of MAR projects in ensuring groundwater resources and raising regional groundwater levels.

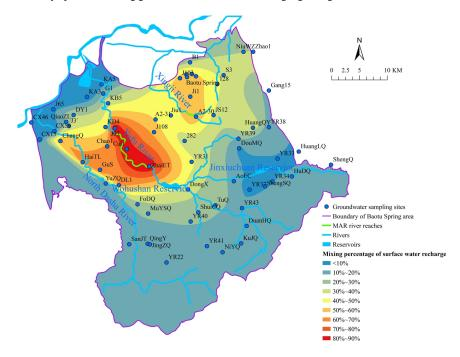


Fig.7 Mixing percentage of surface water recharge in groundwater

## 3.2. Infiltration efficiency of MAR river reaches

According to the test results of in-situ double-ring infiltration test, the bed permeability coefficient of the Yufu River MAR reach ranges from 1.96 to 2.76 m/d, with an average of 2.30 m/d across five sites. According to high-resolution satellite images, the Yufu River MAR reach (Fig.4), from Section #1 to Section #5, approximately covers an area of 0.50 km<sup>2</sup>. Assuming a vertical infiltration hydraulic gradient of 1, the theoretical maximum recharge volume for the Yufu River MAR reach, calculated using



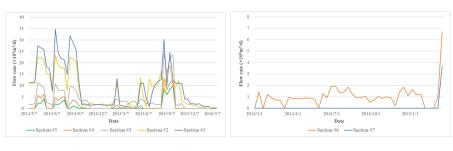


Darcy's Law, is approximately 114.9×10<sup>4</sup>m<sup>3</sup>/d.

Based on field surveys, large volume of released water in the Yufu River results in some flow escaping at the Section #5, failing to infiltrate and recharge karst groundwater, thereby reducing the actual recharge volume. To verify this, analysis of flow data from 2014 to 2016 (Fig.8) was conducted, revealing the relationship between actual recharge volume and released water volume. When the released water volume does not exceed 21.6×10<sup>4</sup>m<sup>3</sup>/d, the actual recharge volume equals the released water volume, indicating full infiltration of surface water before Section #5. However, when the released water volume exceeds 21.6×10<sup>4</sup>m<sup>3</sup>/d, the actual recharge volume is less than the released water volume, as some surface water flows past Section #5 without infiltrating karst groundwater. Calculations confirm that when the released water volume exceeds 21.6×10<sup>4</sup>m<sup>3</sup>/d, the relationship between the actual recharge volume and the released water volume follows formula (7).

$$Q_{Act} = 0.843 \times Q_{Rel} + 3.396$$
 (7)

Where,  $Q_{Act}$  is the actual recharge volume in Yufu River (m<sup>3</sup>/d), and  $Q_{Rel}$  is the released water volume in Yufu River Section #1 (m<sup>3</sup>/d).



329 (a) Yufu River (b) Xingji River

Fig.8 Flow rate curves at various sections of the Yufu River and Xingji River

Likewise, in Xingji River, the relationship between the actual recharge volume and the released water volume follows formula (8) when the released water volume exceeds  $2\times10^4 \text{m}^3/\text{d}$ .





 $Q_{Aci} = 0.214 \times Q_{Rcl} + 1.573$  (8)

Where,  $Q_{Act}$  is the actual recharge volume in Xingji River (m<sup>3</sup>/d), and  $Q_{Rel}$  is the released water volume in Xingji River Section #6 (m<sup>3</sup>/d).

Finally, the actual recharge volume of Yufu River and Xingji River from 2020 to 2022 was calculated in Fig.9, respectively. These calculations were used as surface water recharge inputs for the groundwater flow model.

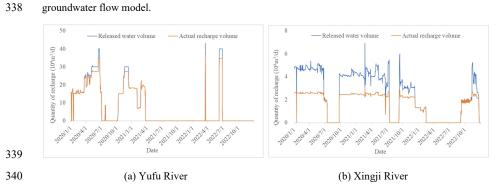


Fig.9 Released water volume VS. Actual recharge volume in Yufu River and Xingji River

#### 3.3. Effective porosity of karst aquifers estimated from tracer tests

As discussed in Section 2.4, the effective porosity at each calculation point was calculated using formula (6), with the process and results shown in Tab.1. Obviously, the effective porosity of the aquifer varies widely, with the maximum, minimum, and average values being  $4.39 \times 10^{-4}$ ,  $1.28 \times 10^{-5}$ , and  $1.08 \times 10^{-4}$ , respectively. This variability is closely related to the heterogeneity of the karst aquifer, aligning with studies in similar carbonate rock regions in the UK and Austria (Medici & West, 2021; Worthington et al., 2019). In this paper, the average effective porosity ( $1.08 \times 10^{-4}$ ) from all calculated points on three flow lines from the Cuima Village and Xingji River tracer tests was used to represent the karst aquifer's effective porosity for groundwater solute transport modeling.





354

355

356

357

Tab.1 Effective porosity at the calculation points

Name	Flow velocity (m/d)	Permeability (m/d)	Hydraulic gradient	Effective porosity
#1-1	233.6	10	4.23E-03	1.81E-04
#1-2	240.3	1	3.85E-03	1.60E-05
#1-3	266.9	2	1.70E-03	1.28E-05
#1-4	295.2	4	1.16E-03	1.58E-05
#1-5	225.5	20	1.20E-03	1.07E-04
#1-6	148.3	20	3.85E-04	5.19E-05
#1-7	82.4	120	3.01E-04	4.39E-04
#1-8	52.4	10	3.07E-04	5.85E-05
#2-1	449.6	10	2.46E-03	5.47E-05
#2-2	293.2	22	1.03E-03	7.70E-05
#2-3	193.5	80	1.67E-04	6.89E-05
#2-4	356.3	80	2.78E-04	6.24E-05
#2-5	307	50	4.42E-04	7.21E-05
#3-1	63	0.3	1.07E-02	5.09E-05
#3-2	96.8	0.3	1.26E-02	3.90E-05
#3-3	165.1	1	1.29E-02	7.83E-05
#3-4	287.7	20	2.08E-03	1.45E-04
#3-5	275.7	120	9.88E-04	4.30E-04
#3-6	71.8	8	8.65E-04	9.64E-05
Max	449.6	/	/	4.39E-04
Min	52.4	/	/	1.28E-05
Average	216	/	/	1.08E-04

# 353 3.4. Impacts of MAR and groundwater exploitation on groundwater level

According to the identification and verification of the groundwater flow model, the horizontal hydraulic conductivity of karst aquifers is exhibited in Fig.10(a). The calculated and observed groundwater flow field as of December 31, 2022, are exhibited in Fig.10(b), and the calculated and observed groundwater levels for representative monitoring wells are shown in Fig.10(c) to 10(f).

359

360

362

364

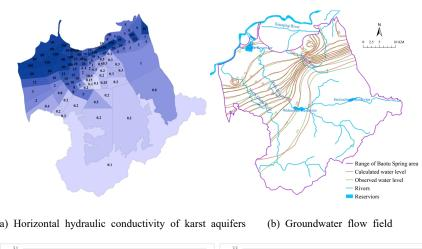
365

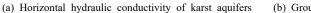
366

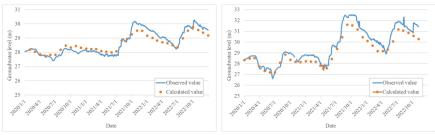
367

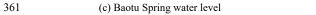
368



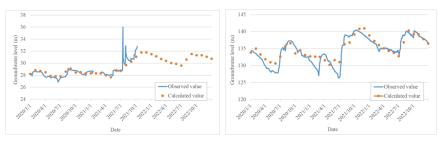








# (d) Qiaozili water level



363 (e) M82 water level (f) A2-30 water level

Fig.10 Identification and verification result of the groundwater flow model

The net variations of Baotu Spring water level caused by MAR and groundwater exploitation were simulated and are displayed in Fig.11. The "net variations of Baotu Spring water level" in Fig.11 refers to the portion of groundwater level fluctuation in Baotu Spring caused by MAR and groundwater exploitation. These variations are calculated using a numerical model based on actual MAR and

377

379

380

381



groundwater exploitation data. It shows that the water level of Baotu Spring clearly rises with MAR and

drops with groundwater exploitation. There is also a lag in the impact of these factors on the water level.

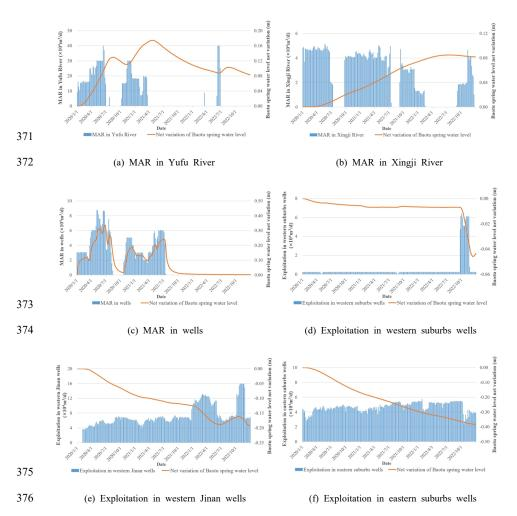


Fig.11 Net variations of Baotu Spring water level caused by MAR and groundwater exploitation (based

378 on data in 2020-2022)

Then, the water level net variation after 1, 2, and 3 years of continuous recharge and exploitation at a constant flow rate was calculated and compared, with detailed results shown in Tab.2. Note that due to maximum recharge capacity constraints, scenarios with recharge volumes of Xingji River and MAR

https://doi.org/10.5194/egusphere-2025-281 Preprint. Discussion started: 10 February 2025 © Author(s) 2025. CC BY 4.0 License.

382

383

384

385

386

387

388

389

390

391

392

393

394

395

396

397

398

399

400

401

402

403





wells exceeding 5×10<sup>4</sup>m<sup>3</sup>/d were not included. Tab.2(a) illustrates the impact of MAR on Baotu Spring's water level. It shows that, with the same recharge volume and duration, the MAR in wells has the greatest effect, followed by Xingji River, and Yufu River has the least impact. Despite this, Yufu River's maximum recharge capacity greatly exceeds that of Xingji River and the MAR wells. Additionally, the water level rise under MAR wells recharge remains almost unchanged within the three years, indicating that the maximum effect is achieved within the first year. This rapid response is due to the proximity of the MAR wells to Baotu Spring (0.75 km, 0.81 km, and 0.35 km, respectively) and the high permeability (k=150 m/d) of the shared karst aquifer. In practice, the most suitable MAR source should be chosen based on the following strategies. Firstly, MAR in wells yields the best results and raises the Baotu Spring water level the fastest, but it has a low maximum recharge capacity. Therefore, MAR in wells should be prioritized for a rapid short-term rise in the Baotu Spring water level. Secondly, MAR in Xingji River is less effective and also has a low maximum capacity, making it suitable for maintaining a small long-term rise in the Baotu Spring water level in conjunction with MAR in wells. Thirdly, MAR in Yufu River is the least effective but has a high maximum capacity, so for a significant long-term rise in the Baotu Spring water level, all three sources should be considered, with MAR in Yufu River being the primary source. Tab.2(b) illustrates the impact of groundwater exploitation on Baotu Spring's water level. Overall, the exploitation in eastern suburbs wells has the most significant impact on Baotu Spring's water level, followed by the western suburbs wells, with the western Jinan wells having the least impact. Between 2020 and 2022, daily average exploitation volume was 5,339 m<sup>3</sup>/d for western suburbs wells, 70,852 m<sup>3</sup>/d for western Jinan wells, and 46,487 m<sup>3</sup>/d for eastern suburbs wells. Therefore, to minimize the impact on the water level of Baotu Spring while ensuring the basic groundwater exploitation needs in the

406

408

409

410

411

412

413

414

415





area, western suburbs wells still hold significant exploitation potential and consideration may be given

405 to transferring a portion of exploitation from eastern suburbs wells to western suburbs wells.

Tab.2 The effect on groundwater level net variation at Baotu Spring resulting from a constant rate of

407 continuous MAR and groundwater exploitation over 1 year, 2 years, and 3 years

### (a). The effect on groundwater level rise resulting from MAR

MAR rate (×10 <sup>4</sup> m <sup>3</sup> /d)		Duration of groundwater recharge		
		1 year	2 years	3 years
	2	19 mm	31 mm	36 mm
	5	49 mm	76 mm	90 mm
Yufu River	10	97 mm	152 mm	179 mm
	20	194 mm	300 mm	353 mm
	30	266 mm	409 mm	480 mm
V::: D:	2	23 mm	60 mm	89 mm
Xingji River	5	38 mm	100 mm	148 mm
MAD 11	2	85 mm	86 mm	86 mm
MAR wells	5	212 mm	214 mm	216 mm

# (b). The effect on groundwater level drop resulting from groundwater exploitation

Groundwater exploitation rate		Duration of groundwater exploitation		
$(\times 10^4 \text{m}^3/\text{d})$		1 year	2 years	3 years
	5	115 mm	138 mm	142 mm
Western suburbs wells	10	230 mm	283 mm	293 mm
TT . T' 11	5	87 mm	106 mm	107 mm
Western Jinan wells	10	175 mm	218 mm	221 mm
	5	199 mm	322 mm	382 mm
Eastern suburbs wells	10	397 mm	643 mm	765 mm

## 3.5. Impacts of MAR on groundwater quality

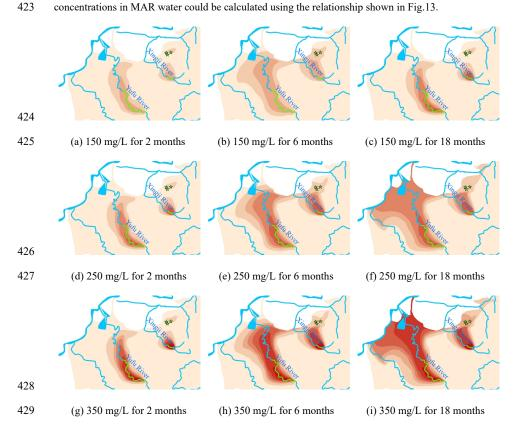
Based on the groundwater solute transport model established in this paper, simulations were conducted to monitor the dynamics of sulphate concentration in karst groundwater after continuous recharge of water with sulphate concentrations of 150 mg/L, 250 mg/L, and 350 mg/L over periods of 2 months, 6 months, and 18 months. As shown in Fig.12, with prolonged recharge duration and deteriorating recharge water quality, the sulphate concentrations in karst groundwater increase and the





affected area of karst groundwater quality expands continuously, indicating an increasing impact of MAR on karst groundwater quality over time. Therefore, deteriorating water quality from MAR poses risks to groundwater, and strict control and monitoring of recharge water quality are necessary.

Additionally, sulphate concentrations in karst groundwater reach stability after 12~18 months of continuous recharge, and a linear regression established a quantitative relationship between the sulphate concentrations in karst groundwater and in MAR water (Fig.13). In practice, target values for sulphate concentrations in karst groundwater should be preset, and the minimum control standards for sulphate concentrations in MAR water could be calculated using the relationship shown in Fig.13.







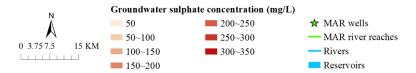


Fig.12 Evolution of sulphate concentration in karst groundwater under MAR

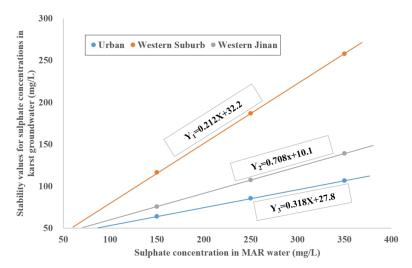


Fig.13 Linear relationships between sulphate concentrations in karst groundwater and MAR water

#### 4. Conclusions

In this research, the impacts of MAR and groundwater exploitation on the dynamics of karst groundwater level and quality in the Baotu Spring area of Jinan City were quantitatively analyzed by multi-methods. The main conclusions are summarized as follows.

Firstly, the  $\delta^2$ H‰ and  $\delta^{18}$ O‰ values of groundwater and surface water reveals that surface water is an essential source of groundwater recharge and plays a crucial role in maintaining groundwater volume. In the southern metamorphic rock and Cambrian Zhangxia Formation limestone outcrop areas, as well as the northwestern Yellow River alluvial plain, the surface water recharge proportion is generally less than 20%. Near the MAR reaches of the Yufu River and Xingji River, the mixing percentage of surface water recharge exceed 80% and 50%, respectively.

445

447

448

449

450

451

453

454

455

457

459

460

461

462

463

464

465





Secondly, according to the analysis of the infiltration test results, the theoretical maximum recharge capacity of the Yufu River to karst groundwater is about 114.9×104m<sup>3</sup>/d by infiltration tests. However, 446 the analysis of the rivers' flow monitoring results reveals that some surface water will flow out downstream when the released water volume of the Yufu River and Xingji River exceeds 21.6×10<sup>4</sup>m<sup>3</sup>/d and 2×104m3/d, respectively, reducing the actual recharge volume. Thirdly, the isoline map of tracer peak concentration diffusion estimated the effective porosity of the karst aquifer in the study area to be  $1.08 \times 10^{-4}$ , providing a reference for solute transport modeling in similar hydrogeological conditions. According to the simulations of the groundwater flow model, 452 MAR effectively raises karst groundwater levels, and the effectiveness varies for the three MAR sources. MAR in wells has the best effect and fastest response, followed by the MAR in Xingji River, though both have low maximum recharge capacities. The MAR from Yufu River has a lower effect but the highest maximum recharge capacity. Furthermore, transferring some amount of the groundwater 456 exploitation from eastern suburbs wells to western suburbs wells might reduce the impact on the water level of Baotu Spring. 458 Finally, poor quality of MAR water would negatively affect karst groundwater, and there is a linear relationship between the concentration of hydrochemical component in MAR water and karst groundwater, allowing for the pre-setting of karst groundwater quality targets and the determination of minimum standards for MAR water quality based on this relationship. In summary, the MAR projects in the Baotu Spring area of Jinan City have significantly impacted the dynamics of karst groundwater level and quality. Proper planning and monitoring of the amount and quality of MAR and groundwater exploitation are essential for maintaining groundwater levels, ensuring continuous spring flow, and safeguarding groundwater quality.

**Statements and Declarations** 

466





467	Data availability
468	The data underlying this article were provided by 801 Institute of Hydrogeology and Engineering
469	Geology, Shandong Provincial Bureau of Geology & Mineral Resources by permission. Data will be
470	shared on request to the corresponding author with permission.
471	Author Contribution
472	The respective contributions of all authors to this paper are as follows:
473	Han Cao: Conceptualization, Methodology, Writing-Original Draft.
474	Weihong Dong: Writing-Review and Editing, Supervision, Project administration.
475	Caiping Hu, Huanliang Chen: Resources, Funding acquisition, Investigation, Data Curation.
476	Jinlong Qian: Investigation, Data Curation.
477	Chunwei Liu, Minghui Lyu, Shuai Gao: Resources, Funding acquisition.
478	Competing Interests
479	The authors have no relevant financial or non-financial interests to disclose.
480	Acknowledgments
481	Many thanks to the sponsoring organizations (801 Institute of Hydrogeology and Engineering
482	Geology, Shandong Provincial Bureau of Geology & Mineral Resources) that made this research possible.
483	Financial support
484	The authors declare that no funds, grants, or other support were received during the preparation of
485	this manuscript.
486	References
487 488 489	Aeschbach-Hertig, W., & Gleeson, T. (2012). Regional strategies for the accelerating global problem of groundwater depletion. <i>Nature Geoscience</i> , <i>5</i> (12), 853-861. <a href="https://doi.org/10.1038/ngeo1617">https://doi.org/10.1038/ngeo1617</a> Ajjur, S. B., & Baalousha, H. M. (2021). A review on implementing managed aquifer recharge in the





- Middle East and North Africa region: methods, progress and challenges. Water International,
   46(4), 578-604. https://doi.org/10.1080/02508060.2021.1889192
- Akurugu, B. A., Obuobie, E., Yidana, S. M., Stisen, S., Seidenfaden, I. K., & Chegbeleh, L. P. (2022).
   Groundwater resources assessment in the Densu Basin: A review. *Journal of Hydrology: Regional Studies*, 40. https://doi.org/10.1016/j.ejrh.2022.101017
- Alam, S., Borthakur, A., Ravi, S., Gebremichael, M., & Mohanty, S. K. (2021). Managed aquifer
   recharge implementation criteria to achieve water sustainability. *Sci Total Environ*, 768, 144992.
   <a href="https://doi.org/10.1016/j.scitotenv.2021.144992">https://doi.org/10.1016/j.scitotenv.2021.144992</a>
- Allocca, V., Manna, F., & De Vita, P. (2014). Estimating annual groundwater recharge coefficient for
   karst aquifers of the southern Apennines (Italy). *Hydrology and Earth System Sciences*, 18(2),
   803-817. https://doi.org/10.5194/hess-18-803-2014
- 501 Bakalowicz, M. (2005). Karst groundwater: a challenge for new resources. *Hydrogeology Journal*, *13*(1), 502 148-160. https://doi.org/10.1007/s10040-004-0402-9
- Cao, H., Dong, W., Chen, H., & Wang, R. (2023). Groundwater vulnerability assessment of typical
   covered karst areas in northern China based on an improved COPK method. *Journal of Hydrology*, 624. <a href="https://doi.org/10.1016/j.jhydrol.2023.129904">https://doi.org/10.1016/j.jhydrol.2023.129904</a>
- Cao, X., Zhang, J., Meng, H., Lai, Y., & Xu, M. (2023). Remote sensing inversion of water quality
   parameters in the Yellow River Delta. *Ecological Indicators*, 155.
   <a href="https://doi.org/10.1016/j.ecolind.2023.110914">https://doi.org/10.1016/j.ecolind.2023.110914</a>
- 509 Craig, H. (1961). Isotopic Variations in Meteoric Waters. *Science (New York, N.Y.)*, *133*(3465), 1702-510 1703. https://doi.org/10.1126/science.133.3465.1702
- Daher, W., Pistre, S., Kneppers, A., Bakalowicz, M., & Najem, W. (2011). Karst and artificial recharge:
   Theoretical and practical problems. *Journal of Hydrology*, 408(3-4), 189-202.
   <a href="https://doi.org/10.1016/j.jhydrol.2011.07.017">https://doi.org/10.1016/j.jhydrol.2011.07.017</a>
- Deng, X., Xing, L., Yu, M., Zhao, Z., Li, C., & Su, Q. (2022). Characteristics of the water cycle of Jinan
   karst spring in northern China. Water Practice and Technology, 17(7), 1470-1489.
   <a href="https://doi.org/10.2166/wpt.2022.075">https://doi.org/10.2166/wpt.2022.075</a>
- Foley, J. A., Ramankutty, N., Brauman, K. A., Cassidy, E. S., Gerber, J. S., Johnston, M., Mueller, N.
  D., O'Connell, C., Ray, D. K., West, P. C., Balzer, C., Bennett, E. M., Carpenter, S. R., Hill, J.,
  Monfreda, C., Polasky, S., Rockstrom, J., Sheehan, J., Siebert, S., Tilman, D., & Zaks, D. P.
  (2011). Solutions for a cultivated planet. *Nature*, 478(7369), 337-342.
  https://doi.org/10.1038/nature10452
- Gao, S., Li, C., Liu, Y., Sun, B., Zhao, Z., Lv, M., & Gang, S. (2023). Hydrogeochemical Characteristics
   and Evolution Processes of Karst Groundwater Affected by Multiple Influencing Factors in a
   Karst Spring Basin, Eastern China. Water, 15(22). https://doi.org/10.3390/w15223899
- Ghasemizadeh, R., Hellweger, F., Butscher, C., Padilla, I., Vesper, D., Field, M., & Alshawabkeh, A.
   (2012). Review: Groundwater flow and transport modeling of karst aquifers, with particular reference to the North Coast Limestone aquifer system of Puerto Rico. *Hydrogeol J*, 20(8),
   1441-1461. <a href="https://doi.org/10.1007/s10040-012-0897-4">https://doi.org/10.1007/s10040-012-0897-4</a>
- Guo, Y., Qin, D., Li, L., Sun, J., Li, F., & Huang, J. (2019). A Complicated Karst Spring System:
   Identified by Karst Springs Using Water Level, Hydrogeochemical, and Isotopic Data in Jinan,
   China. Water, 11(5). <a href="https://doi.org/10.3390/w11050947">https://doi.org/10.3390/w11050947</a>
- Hartmann, A., Goldscheider, N., Wagener, T., Lange, J., & Weiler, M. (2014). Karst water resources in
   a changing world: Review of hydrological modeling approaches. Reviews of Geophysics, 52(3),





- 534 218-242. https://doi.org/10.1002/2013rg000443
- Jiang, X., Lei, M., & Zhao, H. (2019). Review of the advanced monitoring technology of groundwater–
   air pressure (enclosed potentiometric) for karst collapse studies. *Environmental Earth Sciences*,
   78(24). https://doi.org/10.1007/s12665-019-8716-z
- Jourde, H., & Wang, X. (2023). Advances, challenges and perspective in modelling the functioning of
   karst systems: a review. Environmental Earth Sciences, 82(17). <a href="https://doi.org/10.1007/s12665-023-11034-7">https://doi.org/10.1007/s12665-023-11034-7</a>
- Kang, F., Jin, M., & Qin, P. (2011). Sustainable yield of a karst aquifer system: a case study of Jinan
   springs in northern China. *Hydrogeology Journal*, 19(4), 851-863.
   <a href="https://doi.org/10.1007/s10040-011-0725-2">https://doi.org/10.1007/s10040-011-0725-2</a>
- Kidmose, J., Nilsson, B., Klem, N. K., Pedersen, P. G., Henriksen, H. J., & Sonnenborg, T. O. (2023).
   Can effective porosity be used to estimate near-well protection zones in fractured chalk?
   Hydrogeology Journal, 31(8), 2197-2212. https://doi.org/10.1007/s10040-023-02743-1
- Li, C., Zhang, X., Gao, X., Li, C., Jiang, C., Liu, W., Lin, G., Zhang, X., Fang, J., Ma, L., & Zhang, X.
   (2022). Spatial and Temporal Evolution of Groundwater Chemistry of Baotu Karst Water
   System at Northern China. *Minerals*, 12(3). <a href="https://doi.org/10.3390/min12030348">https://doi.org/10.3390/min12030348</a>
- Li, C., Zhao, Y., Liu, W., Liu, C., Jia, C., Wang, C., & Yang, F. (2022). Three-dimensional Digital Core
   Structure Characterization Method and Application of Thick Limestone in Baotu Spring Basin
   of Jinan 2022 8th International Conference on Hydraulic and Civil Engineering: Deep Space
   Intelligent Development and Utilization Forum (ICHCE),
- Li, J., Wang, W., & Li, W. (2023). Total Dissolved Solids Risk Assessment and Optimisation Scheme
   of Managed Aquifer Recharge Projects in a Karst Area of Northern China. Water, 15(22).
   <a href="https://doi.org/10.3390/w15223930">https://doi.org/10.3390/w15223930</a>
- Li, M., Liu, T., Duan, L., Luo, Y., Ma, L., Zhang, J., Zhou, Y., & Chen, Z. (2019). The Scale Effect of
   Double-Ring Infiltration and Soil Infiltration Zoning in a Semi-Arid Steppe. Water, 11(7).
   <a href="https://doi.org/10.3390/w11071457">https://doi.org/10.3390/w11071457</a>
- Li, M., Xie, Y., Dong, Y., Wang, L., & Zhang, Z. (2023). Review: Recent progress on groundwater
   recharge research in arid and semiarid areas of China. *Hydrogeology Journal*, 32(1), 9-30.
   <a href="https://doi.org/10.1007/s10040-023-02656-z">https://doi.org/10.1007/s10040-023-02656-z</a>
- Liang, Y., Gao, X., Zhao, C., Tang, C., Shen, H., Wang, Z., & Wang, Y. (2018). Review: Characterization,
   evolution, and environmental issues of karst water systems in Northern China. *Hydrogeology Journal*, 26(5), 1371-1385. https://doi.org/10.1007/s10040-018-1792-4
- Liu, C., Zhang, G., & Wang, W. (2021). Characteristics of an open karst water system in Shandong
   Province, China. Environmental Earth Sciences, 80(4). <a href="https://doi.org/10.1007/s12665-021-568">https://doi.org/10.1007/s12665-021-568</a>
   09465-1
- Liu, Y., Wang, M., Webber, M., Zhou, C., & Zhang, W. (2020). Alternative water supply solutions:
   China's South-to-North-water-diversion in Jinan. J Environ Manage, 276, 111337.
   <a href="https://doi.org/10.1016/j.jenvman.2020.111337">https://doi.org/10.1016/j.jenvman.2020.111337</a>
- Lorenzi, V., Banzato, F., Barberio, M. D., Goeppert, N., Goldscheider, N., Gori, F., Lacchini, A., Manetta,
   M., Medici, G., Rusi, S., & Petitta, M. (2024). Tracking flowpaths in a complex karst system
   through tracer test and hydrogeochemical monitoring: Implications for groundwater protection
   (Gran Sasso, Italy). Heliyon, 10(2), e24663. <a href="https://doi.org/10.1016/j.heliyon.2024.e24663">https://doi.org/10.1016/j.heliyon.2024.e24663</a>
- Luo, Q., Yang, Y., Qian, J., Wang, X., Chang, X., Ma, L., Li, F., & Wu, J. (2020). Spring protection and
   sustainable management of groundwater resources in a spring field. *Journal of Hydrology*, 582.





- 578 https://doi.org/10.1016/j.jhydrol.2019.124498
- 579 Medici, G., Smeraglia, L., Torabi, A., & Botter, C. (2021). Review of Modeling Approaches to
  580 Groundwater Flow in Deformed Carbonate Aquifers. *Ground Water*, 59(3), 334-351.
  581 <a href="https://doi.org/10.1111/gwat.13069">https://doi.org/10.1111/gwat.13069</a>
- 582 Medici, G., & West, L. J. (2021). Groundwater flow velocities in karst aquifers; importance of spatial 583 observation scale and hydraulic testing for contaminant transport prediction. *Environ Sci Pollut* 584 *Res Int*, 28(32), 43050-43063. https://doi.org/10.1007/s11356-021-14840-3
- Medici, G., West, L. J., Chapman, P. J., & Banwart, S. A. (2019). Prediction of contaminant transport in
   fractured carbonate aquifer types: a case study of the Permian Magnesian Limestone Group (NE
   England, UK). Environ Sci Pollut Res Int, 26(24), 24863-24884.
   <a href="https://doi.org/10.1007/s11356-019-05525-z">https://doi.org/10.1007/s11356-019-05525-z</a>
- Niu, S., Shu, L., Li, H., Xiang, H., Wang, X., Opoku, P. A., & Li, Y. (2021). Identification of Preferential
   Runoff Belts in Jinan Spring Basin Based on Hydrological Time-Series Correlation. *Water*,
   13(22). <a href="https://doi.org/10.3390/w13223255">https://doi.org/10.3390/w13223255</a>
- Ostad-Ali-Askari, K., & Shayannejad, M. (2021). Quantity and quality modelling of groundwater to
   manage water resources in Isfahan-Borkhar Aquifer. *Environment, Development and* Sustainability, 23(11), 15943-15959. https://doi.org/10.1007/s10668-021-01323-1
- Ren, S., Gragg, S., Zhang, Y., Carr, B. J., & Yao, G. (2018). Borehole characterization of hydraulic
   properties and groundwater flow in a crystalline fractured aquifer of a headwater mountain
   watershed, Laramie Range, Wyoming. *Journal of Hydrology*, 561, 780-795.
   https://doi.org/10.1016/j.jhydrol.2018.04.048
- Ringleb, J., Sallwey, J., & Stefan, C. (2016). Assessment of Managed Aquifer Recharge through
   Modeling—A Review. Water, 8(12). <a href="https://doi.org/10.3390/w8120579">https://doi.org/10.3390/w8120579</a>
- Scanlon, B. R., Mace, R. E., Barrett, M. E., & Smith, B. (2003). Can we simulate regional groundwater
   flow in a karst system using equivalent porous media models? Case study, Barton Springs
   Edwards aquifer, USA. *Journal of Hydrology*, 276(1-4), 137-158.
   <a href="https://doi.org/10.1016/s0022-1694(03)00064-7">https://doi.org/10.1016/s0022-1694(03)00064-7</a>
- 605 Sherif, M., Sefelnasr, A., Al Rashed, M., Alshamsi, D., Zaidi, F. K., Alghafli, K., Baig, F., Al-Turbak,
  606 A., Alfaifi, H., Loni, O. A., Ahamed, M. B., & Ebraheem, A. A. (2023). A Review of Managed
  607 Aquifer Recharge Potential in the Middle East and North Africa Region with Examples from
  608 the Kingdom of Saudi Arabia and the United Arab Emirates. *Water*, 15(4).
  609 https://doi.org/10.3390/w15040742
- Standen, K., Costa, L. R. D., & Monteiro, J.-P. (2020). In-Channel Managed Aquifer Recharge: A
   Review of Current Development Worldwide and Future Potential in Europe. Water, 12(11).
   <a href="https://doi.org/10.3390/w12113099">https://doi.org/10.3390/w12113099</a>
- Sun, B. B., Xing, L. T., Li, C. S., Zhang, Y., Wang, L. Y., Zhang, F. J., & Zhou, J. (2013, Apr 13-13).
   Study on Environmental Materials with Analysis of the Hydraulic Connection Between
   Downtown and East and West Suburbs in Jinan, Shandong Province of China. Advanced
   Materials Research [Advanced research on structure, materials and engineering ii]. 2nd
   International Conference on Advanced Structure, Materials and Engineering (ASME 2013),
   Guangzhou, PEOPLES R CHINA.
- Wang, G.-F., Wu, Y.-X., Lu, L., Li, G., & Shen, J. S. (2017). Investigation of the geological and hydrogeological environment with relation to metro system construction in Jinan, China.

  Bulletin of Engineering Geology and the Environment, 78(2), 1005-1024.





622	https://doi.org/10.1007/s10064-017-1140-2
623	Wang, W., Fan, Y., Li, K., Wang, X., & Kang, J. (2022). Challenges of Spring Protection and
624	Groundwater Development in Urban Subway Construction: A Case Study in the Jinan Karst
625	Area, China. Water, 14(9). https://doi.org/10.3390/w14091521
626	Worthington, S. R. H., Foley, A. E., & Soley, R. W. N. (2019). Transient characteristics of effective
627	porosity and specific yield in bedrock aquifers. Journal of Hydrology, 578.
628	https://doi.org/10.1016/j.jhydrol.2019.124129
629	Xanke, J., Liesch, T., Goeppert, N., Klinger, J., Gassen, N., & Goldscheider, N. (2017). Contamination
630	risk and drinking water protection for a large-scale managed aquifer recharge site in a semi-arid
631	karst region, Jordan. Hydrogeology Journal, 25(6), 1795-1809. https://doi.org/10.1007/s10040-
632	<u>017-1586-0</u>
633	Zhang, Z., & Wang, W. (2021). Managing aquifer recharge with multi-source water to realize sustainable
634	management of groundwater resources in Jinan, China. Environ Sci Pollut Res Int, 28(9), 10872-
635	10888. https://doi.org/10.1007/s11356-020-11353-3
636	Zheng, Q. Y., Wang, W. P., Liu, S., & Qu, S. S. (2020). Physical clogging experiment of sand gravel
637	infiltration with Yellow River water in the Yufuhe River channel of Jinan, China [Review].
638	Frontiers of Earth Science, 14(2), 306-314. https://doi.org/10.1007/s11707-019-0772-x
639	Zhu, H., Xing, L., Meng, Q., Xing, X., Peng, Y., Li, C., Li, H., & Yang, L. (2020). Water Recharge of
640	Jinan Karst Springs, Shandong, China. Water, 12(3). https://doi.org/10.3390/w12030694
641	Zuber, A., & Motyka, J. (1994). Matrix porosity as the most important parameter of fissured rocks for
642	solute transport at large scales. Journal of Hydrology, 158(1-2), 19-46.
643	